Research Article | Vol. 29, No. 4 / 15 February 2021 / Optics Express 5598

Optics EXPRESS

Electrically injected GaN-based microdisk towards an efficient whispering gallery mode laser

YANG MEI, MINCHAO XIE, HUAN XU, HAO LONG, LEIYING YING, AND BAOPING ZHANG*

Laboratory of Micro/Nano-Optoelectronics, Department of Micro Electronic and Integrated Circuits, Xiamen University, Xiamen 361005, China
*bzhang@xmu.edu.cn

Abstract: III-nitrides based microdisks with the mushroom-type shape are key components for integrated nanophotonic circuits. The air gap undercut in the mushroom-type microdisk is essential for maintaining vertical optical confinement, but this structure is still facing the difficulty of electrical injection. In this work, we demonstrate an electrically injected GaN-based microdisk of such structure. The device is featured with a copper substrate and copper supporting pedestal, through which current can be efficiently injected into the microdisk with low leakage current (less than 10 nA). Bright emission at ~420 nm was demonstrated from the microdisk under current injection. The copper substrate and supporting pedestal can also extract thermal energy out of the microdisk effectively, and the structure in this work shows a low thermal resistance of ~788.86 K/W. Low threshold lasing action at ~405 nm was realized under the optically pumped condition and the threshold energy is ~35 nJ/pulse. Clear whispering gallery modes were observed and the Q factor is as high as 4504, indicating the high quality of the microdisk cavity. This work is the first step towards low threshold efficient electrically injected microdisk laser with a mushroom-type shape.

1. Introduction

The group III-nitride materials, including those of GaN, AlN, InN, and their mixed alloys, are featured with wide a bandgap and tunable emission spectrum covering from ultraviolet to near infrared [1]. Based on III-nitrides, compact light sources including visible light-emitting diodes (LEDs) and laser diodes (LDs) have already been mass-produced for various applications, such as solid-state lighting [2], multi-color displays [3], and optical data storage [4]. GaN-based microdisk light emitter is a kind of light source featured with low loss and high-quality whispering gallery modes (WGMs), compact small footprint, and low power consumption [5]. It has been intensely pursued for more than decades because of the great potential for both practical application and fundamental researches, such as ultralow threshold microdisk lasers, high efficient micro-LEDs, sensors, as well as linear and nonlinear optics, and strongly coupled cavity quantum electrodynamics [6–10]. Besides, a microdisk light emitter can generate a directional in-plane emission beam through a closely coupled waveguide directly and efficiently, which is of great benefit to on-chip integration [11].

Microdisk light emitter typically has a mushroom-like shape in which the edge is suspended, so that the WGMs could be well confined vertically in the thin microdisk benefiting from the large index difference between semiconductors and air. Based on nitride semiconductors, optically pumped mushroom-type microdisk lasers, sensors, and LEDs fabricated on both Si and sapphire substrate with emission expanding from UVC to green have been successfully demonstrated in the past few years [12–15]. However, GaN-based microdisk with the mushroom type shape is still facing the difficulty of efficient electrical injection. The undercut structure makes it

#416873 https://doi.org/10.1364/OE.416873
Journal © 2021 Received 7 Dec 2020; revised 23 Jan 2021; accepted 1 Feb 2021; published 5 Feb 2021

Optics EXPRESS

difficult to inject current laterally from p-GaN to n-GaN like conventional LED. It is also difficult to inject current vertically from the substrate to microdisk through the supporting pedestal. For microdisks fabricated on sapphire substrate by photoelectron chemical (PEC) etching, the substrate is insulating, and the low-temperature buffer layer in GaN-based microdisk, which is featured with low electrical conductivity and poor material quality, makes it difficult to inject current vertically. The condition is similar in devices on Si substrate. An AlN or AlN/AlGaN multilayer buffer with a high resistivity is commonly grown before GaN to avoid the formation of cracks due to the large lattice difference between GaN and Si. This buffer layer is nearly electrical insulate, blocking the vertically injected current from substrate to GaN microdisk [16].

As a result of the difficulties mentioned above, the electrical injection was realized only in very few cases in GaN-based microdisk cavities or photonic circuits. In 2018, Meixin Feng et al. reported the first electrically injected microdisk laser grown on Si [17]. But the device is featured with a micropillar shape without air undercut so that the epitaxial structure of the microdisk must be specially designed like an edge-emitting laser to confine the WGM inside the nitride membrane. And the current is laterally injected into the microdisk like a conventional LED, which might cause the current crowding effect [18]. In 2019, F. Tabataba-Vakili et al. reported the first electrically injected GaN-based microdisk light emitter on Si with mushroom type shape by using a central buried n-contact to bypass the insulating buffer layers [11]. But the fabrication processes are relatively complicated in this case, and the current injection is still a lateral version. Besides the difficulty of current injection, GaN-based microdisks with mushroom type structure also suffers from the poor heat-sinking capability when compared with micropillar. The heat generated at the periphery of the microdisk can't dissipate efficiently to the substrate because of the air gap, causing a large thermal resistance and high junction temperature.

In this work, we demonstrate an electrically injected GaN-based microdisk with a mushroom-type shape fabricated by a simple new method. The device is featured with a copper substrate and copper supporting pedestal, through which current can be efficiently injected to the nitride microdisk without the current crowding effect, as shown in Fig. 1. Direct bright electroluminescence at ~420 nm was demonstrated under electrical injection. The bias voltage under 20 mA is 5.7 V, and the reverse leakage current under a bias voltage of −5 V is less than 10 nA. Apart from enabling current injection, the copper substrate and supporting pedestal with high thermal conductivity can also extract heat energy out of the microdisk effectively. Thermal characteristics of the mushroom-type microdisk were investigated by using a steady-state quasi three-dimensional cylindrical thermal dissipation model, and the structure in this work shows a

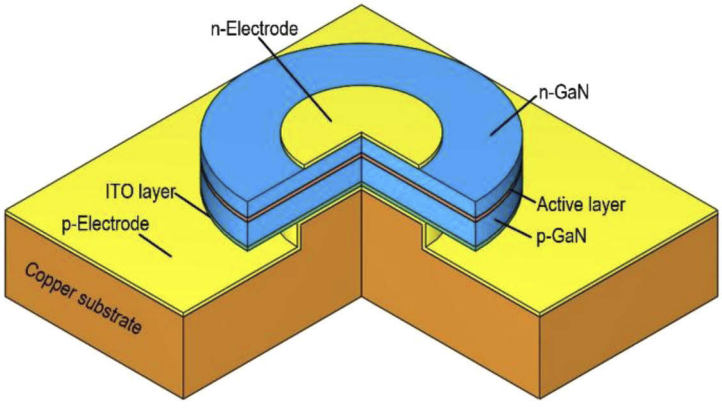

Fig. 1. Schematic structure of the electrically injected microdisk.

Optics EXPRESS

low thermal resistance of ~788.86 K/W. Low threshold lasing action at ~405 nm was realized from the same microdisk under the optically pumped condition and the threshold power is ~35 nJ/pulse. Clear whispering gallery modes were observed and the linewidth of the emission peaks is as narrow as 0.09 nm, inducing a high Q factor of ~4504. This work is the first step towards low threshold efficient electrically injected microdisk WGM laser with mushroom-type shape.

2. Device fabrication

The nitride microdisk is supported by a copper substrate and copper pedestal so that current can be directly injected into the microdisk through the copper substrate and the top electrode. The epitaxial wafer used in this work was grown on (0001)-oriented sapphire substrate by a metal-organic chemical vapor deposition (MOCVD) system. First, a low-temperature buffer layer was grown followed by a 2 μm thick unintentionally doped GaN and a 2 μm thick n-GaN. Then the active region containing five pairs $In_{0.1}Ga_{0.9}N$/GaN (3/5 nm) quantum wells (QWs) was grown followed by a 20 nm thick p-AlGaN electron blocking layer, a 97 nm thick p-GaN, and a 3 nm thick InGaN contacting layer. The fabrication processes of the electrically injected microdisk are depicted schematically in Fig. 2(a). A 120 nm thick indium tin oxide (ITO) film was firstly

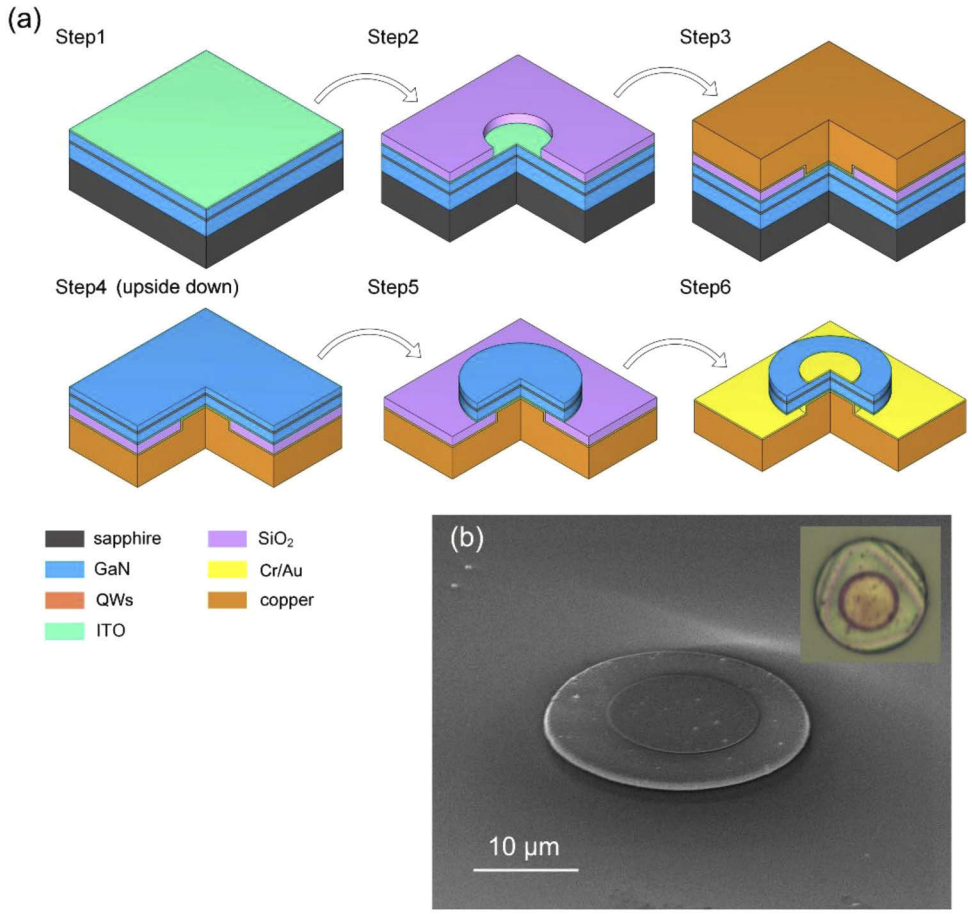

Fig. 2. (a) Process flow of the electrically injected microdisk. The thickness of each layer is not true to scale in order to illustrate the microdisk structure more clearly. (b) SEM image and optical image (inset) of the as-fabricated microdisk.

Optics EXPRESS

deposited on the wafer surface as the current spreading layer (Step 1). Then a 1.5 μm thick SiO_2 layer was deposited, and holes with a diameter of 10 μm were opened to expose the ITO layer (Step 2). After this, a 100 μm thick copper plate was electroplated on the sample surface (Step 3). The holes in the SiO_2 layer was filled by copper, which contacts to the ITO layer and will be the metal supporting pedestal for the semiconductor microdisks in the following steps. Next, the sapphire substrate was removed by the laser lift-off (LLO) process and the nitride membrane was thinned to ~1 μm (Step 4). The microdisks are formed by inductively coupled plasma (ICP) etching, and the etching was stopped while the SiO_2 layer under the nitride membrane was exposed (Step 5). This SiO_2 sacrificial layer is subsequently removed by hydrofluoric acid wet etching so that the mushroom type structure is formed, and a Cr/Au top electrode was deposited on the surface of the microdisks (Step 6). The microdisks are supported by the copper pedestals which are formed during the electroplating process in step 3. The scanning electron microscope (SEM) image as well as the optical image of the as-fabricated mushroom-type microdisk are shown in Fig. 2(b). The height of the supporting copper pedestal is too small (1.5 μm), compared to the size of the upper microdisk (25 μm), to be seen, but the interference pattern in the optical image of the microdisk unambiguously demonstrated the formation of the airgap undercut and the mushroom-type shape. The airgap undercut structure enables the device a much stronger optical confinement when compared with the micropillar type devices.

3. Device performance and discussion

Electroluminescence (EL) characteristics of the device were studied under room-temperature. The cathode and anode probes were placed on the top n-electrode and the copper substrate (p-electrode), respectively, to realize current injection. The emission of the microdisk is collected from the top of the sample with a microscope objective (NA0.35, 10X) and the light is guided through the air into a grating monochromator with an electrical cooled charge-coupled device (CCD) as a detector. Figure 3 shows EL spectra of the device measured under injected currents from 5 to 60 mA. The broad spontaneous emission peak is featured with a centroid wavelength of ~420 nm, and the full width at half maxima (HWFM) is ~30 nm. The centroid wavelength shows a slightly redshift with increasing current, which can be caused by thermal effect. No WGMs were observed and lasing action was not realized under current injection. This can be caused by the fact that the injection level is still not high enough to guarantee the WGMs to obtain sufficient

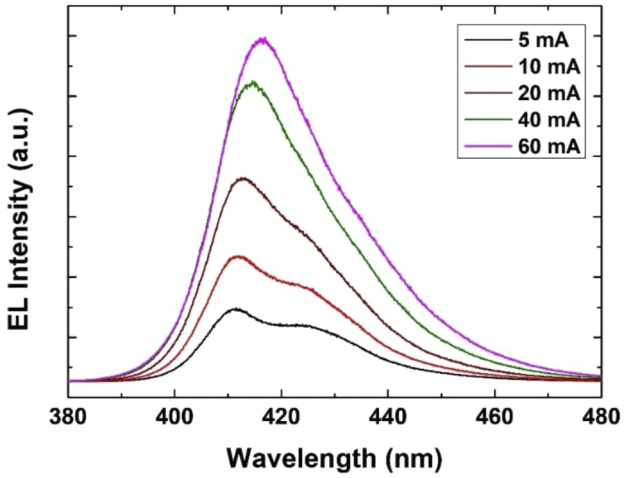

Fig. 3. Emission spectra of the microdisk under different injected currents.

Optics EXPRESS

gain to take dominance over spontaneous emission, and this will be discussed later. Figure 4 shows the typical current versus voltage (IV) curve of a 25 μm diameter microdisk. The bias voltage under 20 mA is 5.7 V, and the reverse leakage current under a bias voltage of −5 V is less than 10 nA (resolution limit of our measurement system), as shown in the inset of Fig. 3. This indicates that the fabrication processes of the electrically injected microdisk do not have any negative influence on the electrical device performance. The insets of Fig. 4 also show the photos of an operating microdisk with bright emission in the violet region under electrical injection.

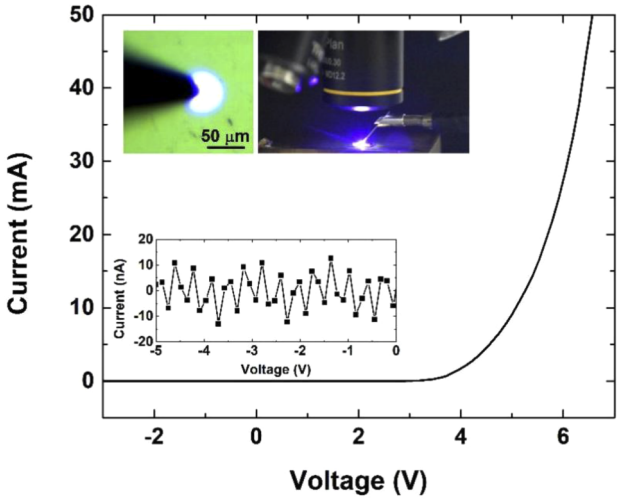

Fig. 4. IV curve of the as-fabricated microdisk. The insets show the reverse-biased IV curve, as well as the photos of an operating microdisk.

The copper substrate and pedestal with high thermal conductivity in the as-fabricated microdisk are expected to effectively improve the thermal dissipation of microdisks with air gap undercut structure. To further investigate the thermal characteristics in such GaN-based mushroom-type microdisks, temperature distribution, and heat flux were studied by finite element method (FEM) using a steady-state quasi three-dimensional (3D) cylindrical heat dissipation model. The detailed information about the thermal dissipation model could be found in our previous work [19]. In this study, the active region was set to be the heat source with a heat source density of ~1.78E15 W/m^3. The heat energy is transferred mainly by conduction to the substrate, and the interfaces between the device and air were assumed to be thermal insulated (no heat transfer). The temperature of the bottom surface of the substrate was set to be room temperature (293.15 K) as a boundary condition during the simulation. The 3D temperature distribution and the corresponding heat flux inside the microdisk are shown in Fig. 5. The temperature near the central region is much lower than that of the periphery region with airgap undercut because of the high thermal conductivity of the copper pedestal (400 W/mK). This large temperature gradient improves thermal dissipation from the periphery to the central region. The maximum temperature inside the active region are 320.76 K, and the increases in temperature, ΔT, is 27.61 K. Then the thermal resistance of the device could be calculated by temperature rise inside the device divided by the power of the heat source to produce heat energy:

$$R_{th} = \frac{\Delta T}{QV}$$

where ΔT, Q, and V are temperature rise, heat source density, and volume of the active region, respectively. The thermal resistance of the device is then turn out to be 788.86 K/W, which is a relatively low value among microdisks with mushroom-type shape. The heat energy in the active

Optics EXPRESS

region can be extracted out of the microdisk more effectively, benefiting from the high thermal conductivity of copper substrate and supporting post. This is essential in electrically injected microdisks with mushroom type structure for the high efficient WGM laser.

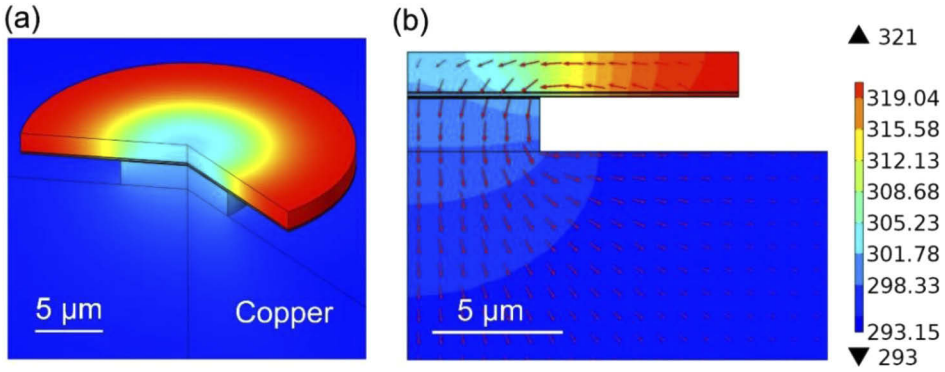

Fig. 5. (a) 3D temperature distribution inside the microdisk. (b) Isotherm surface distribution and heat flux in the cross-sectional slice. The figures are zoomed in to show the microdisk more clearly.

Since lasing was not realized under current injection, to further investigate the optical properties of the microdisk cavity, the device was also measured under optically pumped condition by using a micro photoluminescence system. Single microdisk was excited by a 355 nm pulsed laser with a pulse width of 1 ns and a repeat frequency of 15 kHz. Figure 6(a) shows the emission spectra of the microdisk under different excitation levels. A broad spectrum attributed to spontaneous emission was observed under the excitation energy of 30 nJ/pulse. Then a sharp emission peak emerges at 405.3 nm and increases dramatically when the excitation energy is beyond the threshold. Multi peaks belonging the different WGMs are observed under high excitation energy. The linewidth $\Delta\lambda$ of the emission peaks at around threshold is as narrow as 0.09 nm, inducing a high cavity Q factor of ~4504 obtained by $\lambda/\Delta\lambda$. This indicates the high quality of the as-fabricated microdisk cavity. Figure 6(b) shows the emission intensity as well as the linewidth as a function of excitation energy. The typical "S" shape of the output behavior on the dual logarithmic coordinate and the abrupt reduction of the linewidth prove unambiguously the lasing action and the threshold is as low as 35 nJ/pulse.

Figure 7(a) shows the normalized emission spectra under different excitation levels measured with a grating of high resolution (2400 l/mm). The 405.3 nm cavity mode emerges first and then achieved lasing. More WGMs can be gradually observed with increasing excitation energy, and the lasing peak finally switched to the WGM with a shorter wavelength centered at 402.5 nm. The peaks labeled with black arrows are the first-order (n = 1) WGMs, and the free spectral range (FSR) is ~0.7 nm. FSR of the first order WGMs can be approximately calculated by $FSR = \lambda^2/2\pi n_{eff}R$, where λ (402.3 nm), n_{eff} (2.8 at 402.3 nm), and R (12.5 μm) are mode wavelength, effective index, and radius of the microdisk, respectively. FSR was calculated to be 0.73 nm, consisting well with experimental results. The tiny peaks labeled with red arrows are assumed to be other higher-order WGMs, which are suppressed during spectra evolution when compared with the first order WGMs. This is can be explained by that the radial field distribution of these higher-order modes locates near the center of the microdisk, which will be disturbed by the metallic top electrode and bottom copper pedestal. But the first order modes whose electric field locates near the periphery of the microdisk are not affected. The suppression of the high-order modes will reduce the competition of excited carriers, and can also be a reason for the low threshold lasing of the first-order WGMs. Figure 7(b) shows the mode intensity of the two lasing peaks as a function of excitation energy. The threshold excitation powers is 35 and 67

Optics EXPRESS

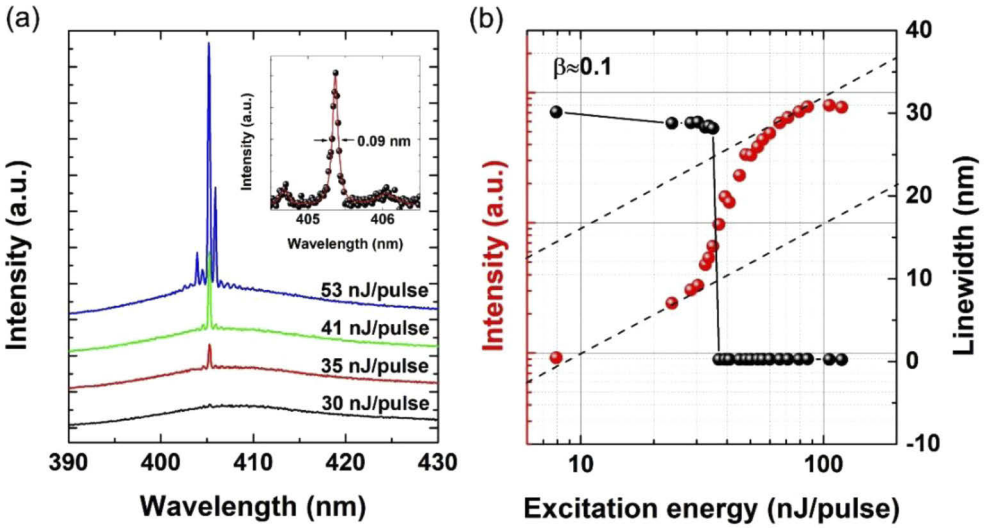

Fig. 6. (a) Emission spectra under different excitation levels. The inset shows the high-resolution spectrum near yhe threshold. (b) Emission intensity as well as linewidth behavior as a function of excitation energy.

nJ/pulse for the 405.3 nm and 402.5 nm WGMs, respectively. The 405.3 nm WGM has a lower threshold, but the 402.5 nm WGM is featured with a much higher slope efficiency.

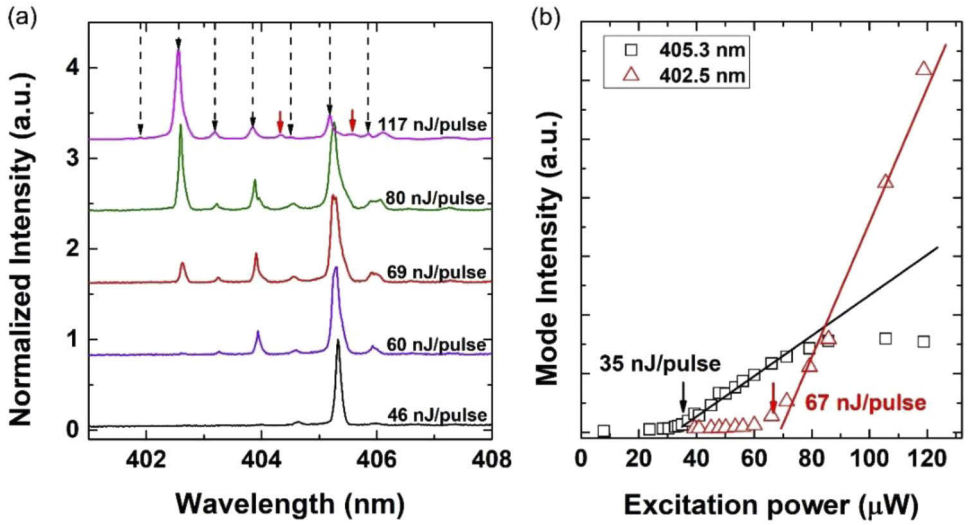

Fig. 7. (a) Normalized emission spectra under different excitation levels. (b) Mode intensity of the 405.3 and 402.5 nm WGMs as a function of excitation energy.

Optically pumped low threshold lasing demonstrated that a microdisk cavity with high quality has been successfully fabricated, which, however, failed to lase under current injection. It is believed that the injection level is still too low to provide the first-order WGMs enough gain to lase. The current is injected into the whole microdisk because of the spreading effect of the ITO layer so that the density of injected carriers is almost equally distributed in the microdisk. The carriers in the central area overlap with the electrical field of the high-order WGMs, and this

Optics EXPRESS

part of injected carriers is of no effect on lasing action because the mode field is disturbed by the metallic electrode and supporting pedestal. On the other hand, the carriers in the peripheral region of microdisk provide gain for the first-order WGMs. However, it is not enough to guarantee lasing action because it takes only a small part of the total injected carriers. Further optimization of device structure such as inserting a current blocking layer between ITO and p-GaN layer to confine injected current to the peripheral region of the microdisk is expected to solve this problem effectively. Although lasing action was not realized under electrically injected condition, the microdisk in this work provides the first step towards achieving a highly efficient electrically injected microdisk laser with a mushroom-type shape for integrated photonics.

4. Conclusion

In this paper, an electrically injected GaN-based microdisk with a new structure was demonstrated. The mushroom-type microdisk is featured with a copper substrate and supporting pedestal so that current injection can be realized efficiently without the current crowding effect. Direct room-temperature bright electroluminescence at ~420 nm was demonstrated. Apart from enabling current injection, the copper substrate and supporting pedestal with high thermal conductivity can also extract heat energy out of the microdisk effectively. And the structure in this work shows a low thermal resistance of ~788.86 K/W. Low threshold lasing action at ~405 nm was realized under the optically pumped condition and the threshold power is as low as ~35 nJ/pulse. The linewidth of the WGMs is ~0.09 nm, inducing a high Q factor of ~4504. This work provides the first step towards achieving a low threshold and efficient electrically injected microdisk laser with a mushroom-type shape for integrated photonics.

Funding. National Key Research and Development Program of China (2016YFB0400803, 2017YFE0131500); National Natural Science Foundation of China (61704140).

Disclosures. The authors declare no conflicts of interest.

References

1. S. Nakamura, T. Mukai, and M. Senoh, "Candela-class high-brightness InGaN/AlGaN double-heterostructure blue-light-emitting diodes," Appl. Phys. Lett. **64**(13), 1687–1689 (1994).
2. M. H. Crawford, "LEDs for solid-state lighting: performance challenges and recent advances," IEEE J. Sel. Top. Quantum Electron. **15**(4), 1028–1040 (2009).
3. Z. Liu, W. C. Chong, K. M. Wong, and K. M. Lau, "GaN-based LED micro-displays for wearable applications," Microelectron. Eng. **148**, 98–103 (2015).
4. H.-c. Yu, Z.-w. Zheng, Y. Mei, R.-b. Xu, J.-p. Liu, H. Yang, B.-p. Zhang, T.-c. Lu, and H.-c. Kuo, "Progress and prospects of GaN-based VCSEL from near UV to green emission," Prog. Quantum Electron. **57**, 1–19 (2018).
5. L. He, Ş. K. Özdemir, and L. Yang, "Whispering gallery microcavity lasers," Laser Photonics Rev. **7**(1), 60–82 (2013).
6. P. Del'Haye, A. Schliesser, O. Arcizet, T. Wilken, R. Holzwarth, and T. J. Kippenberg, "Optical frequency comb generation from a monolithic microresonator," Nature **450**(7173), 1214–1217 (2007).
7. S. Jin, J. Li, J. Li, J. Lin, and H. Jiang, "GaN microdisk light emitting diodes," Appl. Phys. Lett. **76**(5), 631–633 (2000).
8. T. Kouno, K. Kishino, and M. Sakai, "Lasing action on whispering gallery mode of self-organized GaN hexagonal microdisk crystal fabricated by RF-plasma-assisted molecular beam epitaxy," IEEE J. Quantum Electron. **47**(12), 1565–1570 (2011).
9. T. Liu, D. Li, H. Hu, X. Huang, Z. Zhao, W. Sha, C. Jiang, C. Du, M. Liu, and X. Pu, "Piezo-phototronic effect in InGaN/GaN semi-floating micro-disk LED arrays," Nano Energy **67**, 104218 (2020).
10. K. J. Vahala, "Optical microcavities," Nature **424**(6950), 839–846 (2003).
11. F. Tabataba-Vakili, S. Rennesson, B. Damilano, E. Frayssinet, J.-Y. Duboz, F. Semond, I. Roland, B. Paulillo, R. Colombelli, and M. El Kurdi, "III-nitride on silicon electrically injected microrings for nanophotonic circuits," Opt. Express **27**(8), 11800–11808 (2019).
12. I. Aharonovich, A. Woolf, K. J. Russell, T. Zhu, N. Niu, M. J. Kappers, R. A. Oliver, and E. L. Hu, "Low threshold, room-temperature microdisk lasers in the blue spectral range," Appl. Phys. Lett. **103**(2), 021112 (2013).
13. M. Athanasiou, R. Smith, B. Liu, and T. Wang, "Room temperature continuous–wave green lasing from an InGaN microdisk on silicon," Sci. Rep. **4**(1), 7250 (2015).
14. J. Sellés, C. Brimont, G. Cassabois, P. Valvin, T. Guillet, I. Roland, Y. Zeng, X. Checoury, P. Boucaud, and M. Mexis, "Deep-UV nitride-on-silicon microdisk lasers," Sci. Rep. **6**(1), 21650 (2016).

Optics EXPRESS

15. J. Sellés, V. Crepel, I. Roland, M. El Kurdi, X. Checoury, P. Boucaud, M. Mexis, M. Leroux, B. Damilano, and S. Rennesson, "III-Nitride-on-silicon microdisk lasers from the blue to the deep ultra-violet," Appl. Phys. Lett. **109**(23), 231101 (2016).
16. D. Visalli, M. Van Hove, M. Leys, J. Derluyn, E. Simoen, P. Srivastava, K. Geens, S. Degroote, M. Germain, and A. P. D. Nguyen, "Investigation of light-induced deep-level defect activation at the AlN/Si interface," Appl. Phys. Express **4**(9), 094101 (2011).
17. M. Feng, J. He, Q. Sun, H. Gao, Z. Li, Y. Zhou, J. Liu, S. Zhang, D. Li, L. Zhang, X. Sun, D. Li, H. Wang, M. Ikeda, R. Wang, and H. Yang, "Room-temperature electrically pumped InGaN-based microdisk laser grown on Si," Opt. Express **26**(4), 5043–5051 (2018).
18. I. Y. Evstratov, V. Mymrin, S. Y. Karpov, and Y. N. Makarov, "Current crowding effects on blue LED operation," Phys. Status Solidi C **3**(6), 1645–1648 (2006).
19. Y. Mei, R.-B. Xu, H. Xu, L.-Y. Ying, Z.-W. Zheng, B.-P. Zhang, M. Li, and J. Zhang, "A comparative study of thermal characteristics of GaN-based VCSELs with three different typical structures," Semicond. Sci. Technol. **33**(1), 015016 (2018).